ISSN 1023-1935, Russian Journal of Electrochemistry, 2024, Vol. 60, No. 12, pp. 1254–1261. © Pleiades Publishing, Ltd., 2024.

Influence of Metallophilic Interactions on Physicochemical Properties of the Ion-Conducting Glass System $(1 - x)(0.27Sb_2Se_3–0.73GeSe_2)–xAg_2Se$[1]

V. V. Tomaev[a, b, *], Yu. S. Tveryanovich[b, **], S. S. Lun'kov[b], and S. A. Zaitseva[a, b]

[a] *St. Petersburg Institute of Technology (Technical University), St. Petersburg, Russia*

[b] *St. Petersburg State University, St. Petersburg, Russia*

**e-mail: tvaza@mail.ru*

***e-mail: tys@bk.ru*

Received July 1, 2024; revised October 8, 2024; accepted October 30, 2024

Abstract—It is discussed how the silver selenide concentration in glasses of the chalcogenide system $(1 - x)(0.27Sb_2Se_3–0.73GeSe_2)–xAg_2Se$ affects their plasticity, the relationship between microhardness and the softening temperature, and the binding energy of metal atoms in these glasses. Attention is focused on the many-fold increase in plasticity with an increase in the silver selenide content in chalcogenide glasses. These effects are associated with the formation of the metallophilic silver-silver interactions. The results of impedance measurements supplement the studies because the metallophilic interactions in chalcogenide glass can exert a strong effect on the glass transition temperature and many other important properties including the mechanism of electronic and ionic conduction.

Keywords: chalcogenide glass, silver selenide, ionic conductivity, plasticity, metallophilic bonds Ag–Ag, glass network

DOI: 10.1134/S1023193524601505

INTRODUCTION

It is predicted that flexible electronics may induce revolutionary changes in the electronic industry of the 21st century. Hence, of no surprise is the active development of this field [1–3]. Such vigorous changes are due not only to the easiness of using flexible devices in technology but also to the possibility of placing various flexible sensors immediately on the controlled mobile object, e.g., a human body or a dress [4, 5]. In practice, all components of flexible devices including their functional components should sustain repeated mechanical deformations and guarantee structural and functional integrity, including their operation above room temperature [6–8].

It should be noted that the majority of known inorganic semiconductors are brittle at room temperature [9–11] and cannot be used in flexible electronics. This is why the discovery of a semiconductor Ag_2S, flexible at room temperature [12–14] was a breakthrough in solving the long-standing dilemma between mechanical deformability and electric characteristics, which can accelerate the development of flexible electronics [15–17].

The semiconducting materials currently used in flexible electronics can be divided into three main groups: nanocrystalline inorganic [18–20], amorphous inorganic [21–23], and organic substances [24–26]. The nanocrystalline inorganic semiconductors exhibit functional properties but are low-flexible and low-ductile. Organic semiconductors are ductile but their properties rapidly degrade. Amorphous inorganic semiconductors mainly represented by amorphous silicon occupy an intermediate position in this row but have difficult-to-control electronic properties. The ductile glass materials may be considered as a separate group of materials promising for flexible electronics [27–29]. However, glassy materials are as a rule highly brittle, which entails their low resistance to mechanical stresses and temperature variations [30].

At the same time, the chalcogenide glasses with the high silver content were shown to exhibit not only considerable silver-ionic conductivity but also, as demonstrated earlier [31–33], enhanced plasticity as compared with the other chalcogenide glasses. The latter was associated with the ability of silver atoms to form nondirectional metallophillic bonds at their high concentration in the glass network.

On the other hand, it is known that glasses have several advantages over crystals, namely, their properties change slowly with the composition, their ionic conductivity is higher as compared with crystals of the

[1] Based on the report delivered at the 17th International Meeting "Fundamental and Applied Problems of Solid State Ionics", Chernogolovka, June 16–23, 2024

same composition, being disordered systems, they are weakly sensitive with respect to foreign impurities, the modern glass technologies make it possible to fabricate glass issues of any form, etc. [34, 35].

Nonetheless, it is well known that flexible sensors are often fabricated of ductile crystalline inorganic semiconductors based on Ag_2S, Ag_2Se, Ag_2Te [36–38], which pertain to solid electrolytes and are actively studied currently for these purposes.

Generalizing the aforementioned, it can be assumed that glasses capable of incorporating no less than 20 mol % silver chalcogenide without any loss of the glass-forming ability can be considered promising for flexible electronics. The mentioned factors may be responsible for the interest in Ag_2Se-based glass.

In [32], the temperature of glass transition was analyzed for ion-conducting chalcogenide glasses as a function of the silver chalcogenide content. The peculiarities of the changes in the glass-transition temperature for a material based on silver chalcogenides were explained by the coexistence of covalent bonds silver–chalcogen (Al–Ch) and metallophilic bonds silver–silver (Ag–Ag). When assessing the degree of connectivity for the chalcogenide glass network, it is traditionally assumed that the number of bonds formed by each atom coincides with its degree of oxidation. However, it was shown that a large number of chalcogenide glass-forming systems containing silver have a general feature that allowed us to conclude that the connectivity coefficient of silver in chalcogenide glasses substantially exceeds its formal degree of oxidation because silver forms metallophilic bonds in addition to covalent bonds.

Expecting that the metallophilic interactions can affect not only the grass transition temperature but also many other important properties of these glasses including their ionic conductivity, we measured the conductivity as a function of the concentration of silver selenide in glasses of subsystem $(1 - x)(0.27Sb_2Se_3–0.73GeSe_2)–xAg_2Se$.

The choice of this system was associated with the following factors.

The studies of glass in the system $Ag_2Se–Sb_2Se_3–GeSe_2$ [39] convincingly confirmed the assumption that the high coordination of silver in chalcogenide glasses causes the relevant changes in the glass properties, particularly, in the softening temperature T_g. According to these data, the substitution of Ag_2Se for Sb_2Se_3 should substantially increase T_g.

Taking into account that the addition of Ag_2Se to the glass of the $Sb_2Se_3–GeSe_2$ system considerably increases its plasticity [32], we focused our attention on this very system.

Moreover, the concept of the existence of metallophilic bonds in chalcogenide glass is new and, hence, deserves comprehensive investigation and additional confirmation.

According to our results [33] for glass in the system $Ag_2Se–As_2Se_3(Sb_2Se_3)–GeSe_2$, T_g does not decrease with the substitution of Ag_2Se for selenides of even trivalent metals.

The more comprehensive analysis of our results [33] made it possible to assume that it is $GeSe_2$, i.e., the compound containing a metal with the highest coordination number in this glass-forming system, that mainly determines the T_g value. It was also concluded that Ag_2Se in the composition of glass under study renders a similar effect on the T_g value as the effect of selenides of trivalent metals As and Sb. This agrees with the conclusion made in [40] that the average coordination number of atoms in the glassy nanoregions with the Ag_2Se composition is close to 2.4.

The relationship between the plasticity of glass we synthesized in the system $(1 - x)(0.27Sb_2Se_3–0.73GeSe_2)–xAg_2Se$ and the Ag_2Se concentration, which was calculated using the Milman equation [41], can be found in [31]. The observed increase in plasticity can considerably improve the functional properties, particularly, the resistance to temperature variations, and also offers promise for flexible electronics.

Thus, based on this short review of glasses, we have chosen the system $(1 - x)(0.27Sb_2Se_3–0.73GeSe_2)–xAg_2Se$ that exhibits high plasticity and is a candidate for flexible electronics.

This study is aimed at the further development of the concept of metallophilic interactions of silver atoms in chalcogenide glasses, the investigation of their effect on the energy of interatomic interactions using the XRD method, and also on the ion transport using impedance spectroscopy. These results are discussed based on the experimental data on the softening temperature and the plasticity of glasses.

MATERIALS AND METHODS

Glass synthesis (GS). Chalcogenide glasses were synthesized based on elemental substances using the method described in [42] and contained the following amounts of the main components: Sb (99.995%), Se (99.997%), Ag (99.990%), and Ge (99.999%). The following compositions were synthesized: (0) $x = 0.00$; (1) $x = 0.05$; (2) $x = 0.10$; (3) $x = 0.15$; (4) $x = 0.20$; (5) $x = 0.25$; (6) $x = 0.30$; (7) $x = 0.35$; (8) $x = 0.40$; (9) $x = 0.45$. For this purpose, the components of the required composition were placed into quartz ampoules. Then, the ampoules were evacuated to a pressure of 10^{-4} mm Hg and sealed. This guaranteed the invariance of the glass composition during the synthesis. For all compositions, the synthesis was carried out using a muffle furnace at 900°C for 3 h at constant agitation. To increase the cooling rate, the ampoules were placed into ice water immediately after the synthesis. All the methods used here, except for impedance spectroscopy, placed no requirements on the sample form. The samples for impedance spectros-

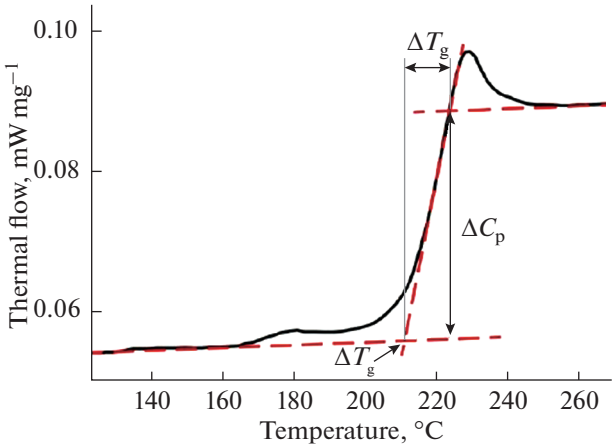

Fig. 1. DSC curve of a glass sample with $x = 0.30$. It is shown how one can determine the values of T_g, ΔC_p, and ΔT_g from this curve.

copy were annealed and then trimmed to obtain flat-parallel plates of 3 mm thickness.

X-ray diffraction (XRD). The X-ray diffraction analysis of all synthesized glasses was carried out according to [42] using a diffractometer ARL X'TRA in the mode of θ–2θ scanning (CuK_α radiation, λ = 1.541 Å) in the interval 2θ = 20°–60°, in steps of 0.04°, at the exposure of 2 s per point. This method, despite the controversial views on its usefulness for studying the glass structure, was taken into consideration by scientists for a long time [43, 44].

Differential scanning calorimetry (DSC). T_g of the glasses was measured using a high-performance differential scanning calorimeter Netzsch DSC 204 F1 Phoenix with a μ sensor [45]. The design of the measuring chamber provided the uniform heating of the μ-sensor disk aimed at obtaining a stable and reproducible baseline and had an efficient cooling system. The glasses of the studied compositions were preliminarily crushed in an agate mortar and placed into an aluminum crucible. The analysis was carried out in the temperature interval of 30–350°C, the heating rate was 10 deg/min.

In addition to the high accuracy in temperature measurements, the μ sensor provided a high sensitivity level never reached earlier in calorimetry.

X-ray photoelectron spectroscopy (XPS). Photoelectron spectroscopy based on the photoeffect phenomenon is a modern method of studying the populated electronic states in solids and can provide additional information on the properties of studied glasses [46].

The XPS studies of glass of the above compositions were carried out using an analytical XPS module Nanolab and a complex photoelectron–scanning Auger spectrometer Thermo Fisher Scientific Escalab 250Xi.

Impedance spectroscopy (IS). The impedance spectroscopic measurements of the glasses studied here were carried out using an impedance meter Elins Z-1000P (Elins, Russia) in a two-contact cell with reversible Ag electrodes in the frequency range of 1–10^6 Hz [47]. Glass samples shaped as cubes with 3 mm edges were thoroughly polished. The silver paste was placed on the opposite faces of all glasses to serve as the reversible electrodes. All impedance hodographs were processed using a special program ZView and the graphics software Origin (Origin). Based on the obtained data, the resistance and the specific conductance of samples were determined.

RESULTS AND DISCUSSION

The introduction of univalent metals into the composition of chalcogenide glass led to a decrease in the average number of bonds per atom. Thus, the connectivity of the glass network decreased. This resulted in the fast decrease of T_g. As the concentration of Ag_2Se increased to 20 mol %, it became possible for silver atoms to form not only covalent bonds with selenium but also the metallophilic interactions with one another. This substantially decelerated the decrease in T_g. As a result, the glass containing 40 mol % Ag_2Se had $T_g = 200$°C. This is higher than the softening temperature of such classical chalcogenide glasses as As_2S_3 and As_2Se_3.

Glass synthesis. All synthesized glasses were black and had a characteristic blistered cleavage.

X-ray diffraction analysis. According to the results of XRD analysis of all glasses synthesized in this system, their diffraction patterns contained only wide amorphous peaks (halos) typical of glassy materials, which confirmed the absence of crystalline inclusions. One exclusion was sample 9 which included crystalline phases, according to XRD data.

Differential scanning calorimetry (DSC). Figure 1 shows a DSC curve for a sample of glass with $x = 0.30$. The glass softening effect was observed with good resolution which allowed us (as shown in Fig. 1) to analyze also the concentration dependences for the quantities other than the glass softening temperature (T_g).

Figure 2 shows the dependence of the glass transition temperature on the concentration of Ag_2Se. The value of T_g for a glass containing no Ag_2Se was 280°C which adequately agrees with the literature data [48].

Photoelectron spectroscopy. The X-ray photoelectron spectra of all elements (except for Ag spectra) contained several lines. Thus, after the deconvolution of spectrum, we calculated the concentration dependence of the weight-average binding energy of the whole spectrum for each element using the equation

$$E_s = \frac{\sum_i E_i A_i}{\sum_i A_i},$$

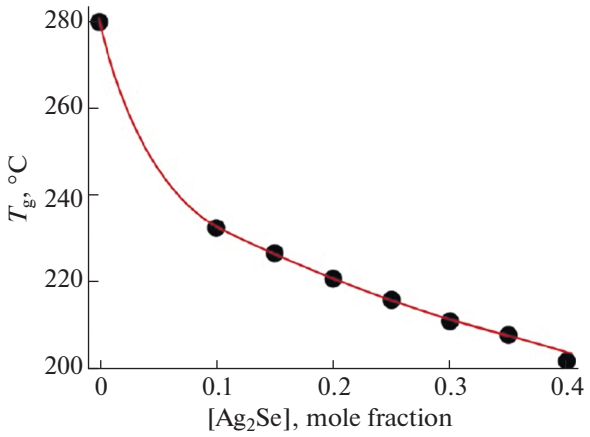

Fig. 2. Dependence of the glass transition temperature determined by the DSC method on the Ag_2Se concentration in glasses of the studied system.

where E_i is the position of the maximum of the ith band in the spectrum; A_i is its integral relative intensity.

Figure 3 shows the dependences of the binding energy (E_s) for each element involved in the glass composition on the Ag_2Se concentration.

Based on these results, the following assumptions can be drawn.

The binding energy of Sb (Fig. 3a) was almost independent of the glass composition. The binding energies of the other elements (Figs. 3b–3d) increased with an increase in the silver content. In this case, the ratio of concentrations of antimony and germanium selenides remained unchanged. Hence, we can assume that the changes were indeed associated with the increase in the Ag_2Se content.

The XRD analysis revealed no crystalline inclusions in glass with $x \le 0.4$. At $x = 0.45$, the crystalline inclusions of the compound Ag_8GeSe_6 appeared. Hence, we can assume that the increase in E_s for Ag, Ge, Se is a result of the formation of ternary structural units of this compound in the glass network. However, the content of $GeSe_2$ in the glass with $x = 0$ was high (73 mol %). This is why even for the initial additions of Ag_2Se, the formation of structural units of compound Ag_8GeSe_6 met no complications and E_s^{Ag} should not depend on the composition. On the other hand, E_s^{Ge} should increase linearly with an increase in the Ag_2Se content. As to the observed variations in the E_s for Ag, Ge, and Se, they demonstrated the zero derivative at

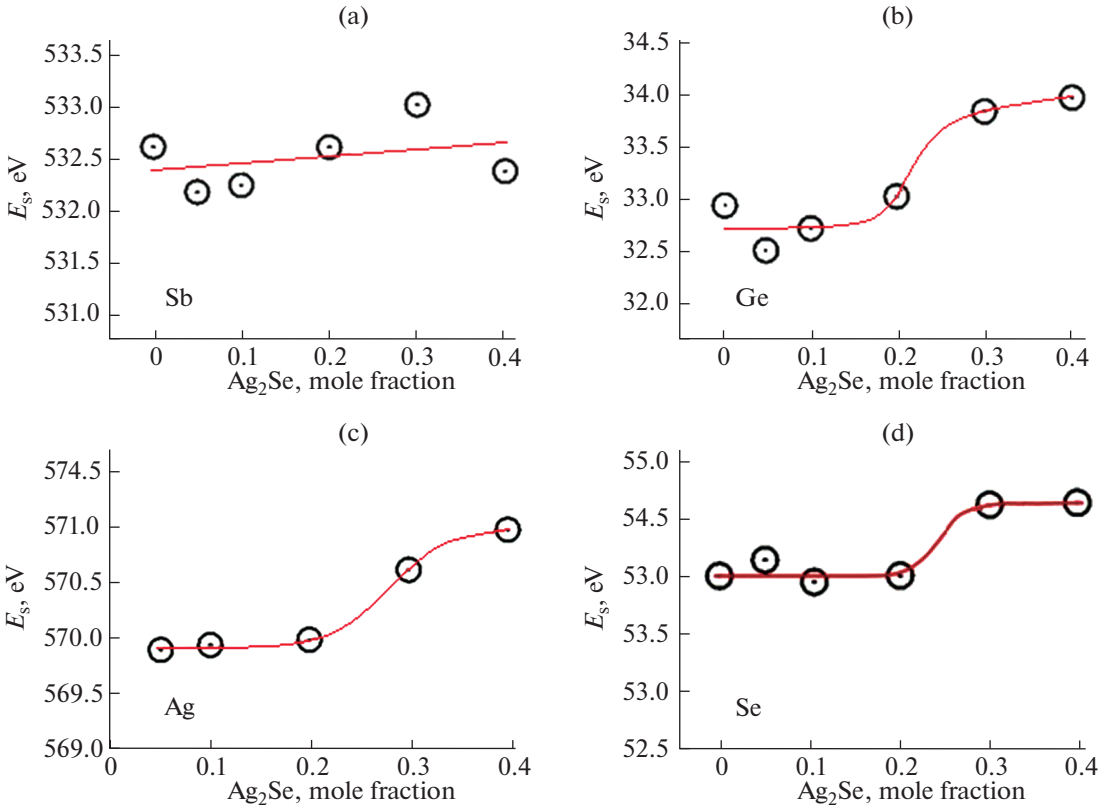

Fig. 3. Dependence of the weight-average binding energy of each element in glasses of the system $(1 - x)(0.27Sb_2Se_3–0.73GeSe_2)–xAg_2Se$ on the Ag_2Se concentration.

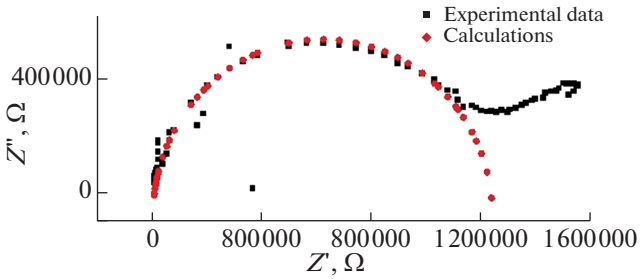

Fig. 4. Dependence of the imaginary part of impedance on its real part for glass with $x = 0.4$. Black symbols are the experimental data, red symbols are the result of approximation.

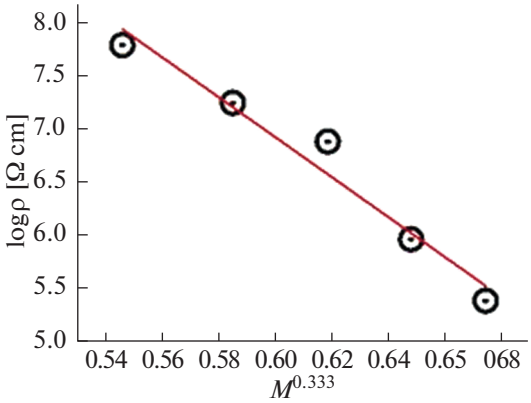

Fig. 5. Dependence of the logarithm of specific resistance of glass in the system $(1 - x)(0.27Sb_2Se_3–0.73GeSe_2)–xAg_2Se$ on the cubic root of the atomic fraction of silver.

the low content of Ag_2Se. This means that this effect is described by a power dependence on the Ag_2Se content with the power index not lower than 2. The metallophilic interactions Ag–Ag comply with this requirement.

Thus, E_s^{Ag} increases with the increase in the silver content due to metallophilic interactions Ag–Ag. Moreover, this increase extends by the induction mechanism to the elements localized in the first and second coordination spheres of silver. These are selenium and germanium. Antimony is not among these elements, so that the structural units of this compound based on Ag, Ge, and Se do not include Sb. The individual crystalline phase of this compound forms at the alloy crystallization when the critical content of Ag_2Se is exceeded.

Impedance spectroscopy. The measured dependences of impedance's imaginary part Z'' on its real part Z' are typical of solid electrolytes (Fig. 4).

Using these results, the experimentally obtained values of the specific active resistance were assigned to the ionic conductivity.

Based on the results of impedance spectroscopy, the dependence of the specific resistance on the Ag_2Se content in the glass (x) was found. According to relationships proposed for describing the transport of single-charged cations in chalcogenide glass [49, 50], $\log R \sim \sqrt[3]{M}$ (where R is the specific resistance, M is the atomic fraction of the single-charged cation). The experimental results plotted in these coordinates (Fig. 5) comply with this relationship.

Furthermore, the extrapolation of this dependence to a silver concentration that corresponded to the Ag_2Se composition gave the specific resistance of 54 Ω cm. Taking into account that we dealt not with a crystalline compound of this composition but with a hypothetical glass, this value of specific resistance was considered reasonable.

The impedance hodographs represented semicircumferences with the center below abscissa. It is well known that this is due to the fluctuational scatter in the characteristic time τ that describes the corresponding hodograph (the reciprocal of the voltage frequency corresponding to the maximum imaginary part of the hodograph). The wider the τ scatter, the lower is the circumference center in the hodograph. The fluctuational character is inherent to the glassy state.

The τ fluctuations can be compared with the fluctuations of potential barriers the cations overcome during their migration. The value of these frozen fluctuations is determined by the glass formation temperature (T_g). For the studied glasses with x varying from 0.2 to 0.4, the deviation of T_g from the average value was ±2% in this concentration interval. This allowed us to assume that the fluctuation of the potential barrier height was constant. The height itself, being dependent of the Ag_2Se concentration, changed substantially giving rise to considerable changes in the logarithm of specific resistance. Hence, we can conclude that the relative role of the τ fluctuations should increase with an increase in the Ag_2Se concentration and a decrease in R.

The parameter that determines numerically, independently of the specific resistance value, the shift of the circumference center (and, hence, the τ fluctuations) is the tangent of the angle (tanα) formed by abscissa and the circumference radius drawn to intersection with abscissa.

Figure 6 shows the dependence of logarithm of tan α on logarithm of specific resistance.

As expected, the increase in the specific resistance of glass was accompanied by a decrease in the role of fluctuational scatter of the characteristic times of hodographs.

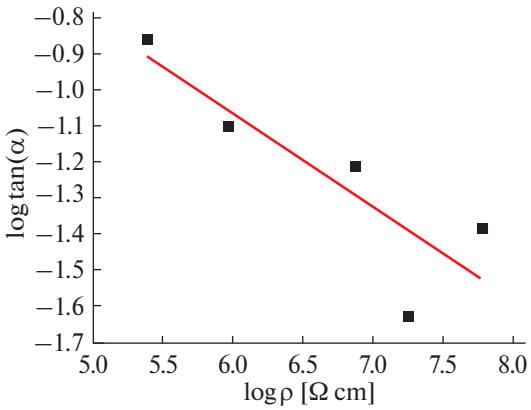

Fig. 6. Dependence of logarithm of tan α on logarithm of specific resistance of glass in the system $(1 - x)(0.27Sb_2Se_3–0.73GeSe_2)–xAg_2Se$.

CONCLUSIONS

The experimental results, in particular, the threshold nature of the increase in the binding energy of Ge, Se, and Ag with an increase in the Ag content confirm the formation of metallophilic bonds Ag–Ag in glass of the system $(1 - x)(0.27Sb_2Se_3–0.73GeSe_2)–xAg_2Se$ for the Ag_2Se concentration above 20 mol %. At the same time, no peculiarities are observed in the behavior of the concentration dependence of the ionic conductivity. Apparently, this is associated with the following factors. Ag_2Se and chalcogenide glasses in general, including glasses of the system under consideration, are formed by covalent chemical bonds metal–chalcogen with the ionic fraction of less than 10%. This is why, there is no strong coulomb interaction between silver atoms, which allows them to come closer to one another and form metallophilic interactions. To participate in the ion transport, an Ag atom should acquire an electric charge and hence break the metallophilic interaction. Thus, the metallophilic interaction has no effect on the transport of Ag ions. However, we cannot rule out its contribution to the process of the transition of silver atoms from the covalent state with the minimum effective charge to the state with the integer charge that takes part in the ion transport.

ABBREVIATIONS AND NOTATION

Ch	chalcogen
T_g	softening (glass transition) temperature
XRD	X-ray diffraction
DSC	differential scanning calorimetry
XPS	X-ray photoelectron spectroscopy
IS	impedance spectroscopy
C_p	heat capacity
E_s	binding energy
E_i	position of the maximum of the ith band in the spectrum
A_i	integral relative intensity of the ith band
Z' and Z''	real and imaginary parts of impedance
R	specific resistance
M	atomic fraction of the single-charged cation
τ	characteristic time
α	angle between abscissa and circumference's radius

ACKNOWLEDGMENTS

The properties of materials were experimentally studied in the Research Park of the St. Petersburg State University (Interdisciplinary Research Centers on Nanotechnology, X-ray Diffraction, Thermogravimetry, Physical Methods for Studying Surfaces, Diagnostics of Functional Materials for Medicine, Pharmacology, and Nanoelectronics) and also in the Engineering Center of the St. Petersburg Technological Institute (Technical University).

FUNDING

This study was supported by the Russian Scientific Foundation (grant no. 24-23-001400).

CONFLICT OF INTEREST

The authors of this work declare that they have no conflict of interest.

REFERENCES

1. Chen, K., Pan, J., Yin, W., Ma, C., and Wan, L., Flexible electronics based on one-dimensional inorganic semiconductor nanowires and two-dimensional transition metal dichalcogenides, *Chin. Chem. Lett.*, 2023, vol. 34, 108226, 16 p.
2. Chen, H., Wei, T.-R., Zhao, K., Qiu, P., Chen, L., He, J., and Shi, X., Room-temperature plastic inorganic semiconductors for flexible and deformable electronics, *InfoMat*, 2021, vol. 3, p. 22.
3. Li, H., Cao, Y., Wang, Z., and Feng, X., Flexible and stretchable inorganic optoelectronics, *Opt. Mater. Express*, 2019, vol. 9, no. 10, p. 4024.
4. Gao, W., Ota, H., Kiriya, D., Takei, K., and Javey, A., Flexible electronics toward wearable sensing, *Acc. Chem. Res.*, 2019, vol. 52, p. 523.
5. Hu, J., Dun, G., Geng, X., Chen, J., Wu, X., and Ren, T.-L., Recent progress in flexible micro-pressure sensors for wearable health monitoring, *Nanoscale Adv.*, 2023, vol. 5, p. 3131.
6. Kim, J., Lee, J., Son, D., Choi, M.K., and Kim, D.-H., Deformable devices with integrated functional nanomaterials for wearable electronics, *Nano Convergence*, 2016, vol. 3, no. 4, p. 13.

7. Vu, C.C., Kim, S.J., Kim, J., Flexible wearable sensors—an update in view of touch-sensing, *Sci. and Technol. Adv. Mater.*, 2021, vol. 22, no. 1, p. 26.
8. Amani, A.M., Tayebi, L., Abbasi, M., Vaez, A., Kamyab, H., Chelliapan, S., and Vafa, E., The need for smart materials in an expanding smart world: MXene-based wearable electronics and their advantageous applications, *ACS Omega*, 2024, vol. 9, no. 3, p. 3123.
9. Pisula, W., Inorganic semiconductors in electronic applications, *Electron. Mater.*, 2023, vol. 4, p. 136.
10. Wang, S., Sun, M., and Hung, N.T., Advanced inorganic semiconductor materials, *Inorganics*, 2024, vol. 12, p. 81.
11. Sun, Y. and Rogers, J.A., Inorganic semiconductors for flexible electronics, *Adv. Mater.*, 2007, vol. 19, p. 1897.
12. Shi, X., Chen, H., Hao, F., Liu, R., Wang, T., Qiu, P., Burkhardt, U., Grin, Y., and Chen, L., Room-temperature ductile inorganic semiconductor, *Nat. Mater*, 2018, vol. 17, p. 421.
13. Liang J., Wang T., Qiu P., Yang S., Ming C., Chen H., Song Q., Zhao K., Wei T.-R., Ren D., Sun Y.-Y., Shi X., He J., Chen L., Flexible thermoelectrics: from silver chalcogenides to full-inorganic devices, *Energy Environ. Sci.*, 2019, vol. 17, no. 8, p. 9.
14. Min, Zhu, Xiao-Lei, Shi, Hao, Wu, Qingfeng, Liu, and Zhi-Gang, Chen, *Advances in Ag_2S-based thermoelectrics for wearable electronics: Progress and perspective*, *Chem. Eng. J.*, 2023, vol. 475, p. 146194. 17 p.
15. Sadovnikov, S.I., Kostenko, M.G., Gusev, A.I., and Lukoyanov, A.V., Low-temperature predicted structures of Ag_2S (silver sulfide), *Nanomaterials*, 2023, vol. 13, p. 2638.
16. Ge, B., Li, R., Zhu, M., Yu, Y., and Zhou, C., *Deformation mechanisms of inorganic thermoelectric materials with plasticity*, *Adv. Energy Sustainability Res.*, 2024, vol. 5, p. 2300197. 11 p.
17. Zhu, Y., Liang, J.-S., Shi, X., and Zhang, Z., Full-inorganic flexible Ag_2S memristor with interface resistance–switching for energy-efficient computing, *ACS Appl. Mater. Interfaces*, 2022, vol. 14, p. 43482.
18. *Flexible Electronics: Materials and Applications*, Wong, W.S. and Salleo, A., Eds., New York: Springer, 2009.
19. Kim, D.-H., Lu, N., Ghaffari, R., and Rogers, J.A., Inorganic semiconductor nanomaterials for flexible and stretchable bio-integrated electronics, *NPG Asia Mater.*, 2012, vol. 4, p. 9.
20. Wang, C., Cheng, R., Liao, L., and Duan, X., High performance thin film electronics based on inorganic nanostructures and composites, *Nano Today*, 2013, vol. 8, p. 514.
21. Jang, H.-J., Lee, K. J., Jo, K.-W., Katz, H. E., Cho, W.-J., and Shin, Y.-B., Top-down fabrication and enhanced active area electronic characteristics of amorphous oxide nanoribbons for flexible electronics, *Sci. Rep.*, 2017, vol. 7, p. 5728.
22. Martinez, R.V., Flexible electronics: Fabrication and ubiquitous integration, *Micromachines*, 2018, vol. 9, p. 605.
23. Gupta, S., Navaraj, W. T., Lorenzelli, L., and Dahiya, R., Ultra-thin chips for high-performance flexible electronics, *npj Flex Electron.*, 2018, vol. 8, p. 17.
24. Li, L., Han, L., Hu, H., and Zhang, R., A review on polymers and their composites for flexible electronics, *Mater. Adv.*, 2023, vol. 4, p. 726.
25. Ling, H., Liu, S., Zheng, Z., and Yan, F., *Organic flexible electronics*, *Small Methods*, 2018, vol. 2, p. 1800070. 33 p.
26. Liu, H., Liu, D., Yang, J., Gao, H., and Wu, Y., *Flexible electronics based on organic semiconductors: From patterned assembly to integrated applications*, *Small*, 2023, vol. 19, p. 2206938. 27 p.
27. Wang, X., He, F., Zimmer, J., US Patent 2016/0002103 A1, 2016.
28. Langgemach, W., Baumann, A., Ehrhardt, M., Preußner, T., and Rädlein, E., The strength of uncoated and coated ultra-thin flexible glass under cyclic, *AIMS Mater. Sci.*, 2024, vol. 11, no. 2, p. 343.
29. Garner, S., Glaesemann, S., and Li, X., Ultra-slim flexible glass for roll-to-roll electronic device fabrication, *Appl. Phys. A*, 2014, August. https://doi.org/10.1007/s00339-014-8468-2
30. Yan, J., Zhou, T., Masuda, J., and Kuriyagawa, T., Modeling high-temperature glass molding process by coupling heat transfer and viscous deformation analysis, *Precision Engineering*, 2009, vol. 33, p. 150.
31. Tveryanovich, Y.S., Fazletdinov, T.R., Tverjanovich, A.S., Fadin, Y.A., and Nikolskii, A.B., Features of chemical interactions in silver chalcogenides responsible for their high plasticity, *Russ. J. Gen. Chem.*, 2020, vol. 90, no. 11, p. 2203.
32. Tveryanovich, YuS., Fazletdinov, T. R., Tverjanovich, A.S., Pankin, D.V., Smirnov, E.V., Tolochko, O.V., Panov, M.S., Churbanov, M.F., Skripachev, I.V., and Shevelko, M.M., Increasing the plasticity of chalcogenide glasses in the system $Ag_2Se–Sb_2Se_3–GeSe_2$, *Chem. Mater.*, 2022, vol. 34, no. 6, p. 2743.
33. Tveryanovich, Yu.S., Fazletdinov, T R., and Tomaev, V.V., Peculiarities of the effect of silver chalcogenides on the glass-formation temperature of chalcogenide glasses with ionic conduction, *Russ. J. Electrochem.*, 2023, vol. 59, no. 8, p. 567.
34. Borisova, Z., *Glassy Semiconductors*, Springer US, 1981, 506 p.
35. Tveryanovich, Yu.S., Some ideas in chemistry and physics of chalcogenide glass, *International year of glass in Russia* (Proc. Scientific Conf.), 2022, p. 147. ISBN 978-5-906224-14-9.
36. Yang, D., Shi, X.-L., Li, M., Nisar, M., Mansoor, A., Chen, S., Chen, Y., Li, F., Ma, H., Liang, G. X., Zhang, X., Liu, W., Fan, P., Zheng, Z., and Chen, Z.-G., Flexible power generators by Ag_2Se thin films with record-high thermoelectric performance, *Nat. Commun.*, 2024, vol.1, no. 5, p. 923. 11 p.
37. Yang, Q., Yang, S., Qiu, P., Peng, L., Wei, T.-R., Zhang, Z., Shi, X., and Chen, L., Flexible thermoelectrics based on ductile semiconductors, *Science*, 2022, vol. 377, no. 8, p. 854.
38. Evarestov, R.A, Panin, A.I, and Tverjanovich, Y.S., Argentophillic interactions in argentum chalcogenides: First principles calculations and topological analysis of electron density, *J. Comput. Chem.*, 2021, vol. 42, no. 4, p. 242.

39. Vassilev, V.S., Boycheva, S.V., and Ivanova, Z.G., Glass formation and physicochemical properties of the $GeSe_2$–Sb_2Se_3–Ag_2Se(ZnSe) systems, *J. Mater. Sci. Lett.*, 1998, vol. 17, p. 2007.

40. Olekseyuk, I.D., Kogut, Yu.M., Parasyuk, O.V., Piskach, L.V., Gorgut, G.P., Kus'ko, O.P., Pekhnyo, V.I., and Volkov, S.V., Glass-formation in the Ag_2Se–Zn(Cd,Hg)Se–$GeSe_2$ systems, *Chem. Met. Alloys*, 2009, vol. 2, p. 146.

41. Milman, Y.V., Galanov, B.A., and Chugunova, S.I., Plasticity characteristic obtained through hardness measurement, *Acta Metall. Mater.*, 1993, vol. 41, no. 9, p. 2523.

42. Tveryanovich, Y.S., Fokina, S.V., Borisov, E.N., and Tomaev, V. V., Preparation of films of vitreous solid electrolyte $(GeSe_2)_{30}(Sb_2Se_3)_{30}(AgI)_{40}$ using laser ablation method, *Glass Phys Chem.*, 2015, vol. 41, p. 440.

43. Tomaev, V.V., Tveryanovich, Yu.S., Balmakov, M.D., Zvereva, I.A., and Missyul, A.B., Ionic conductivity of $(As_2Ss_3)_{1-x}(AgHal)_x$ (Hal = I, Br) nanocomposites, *Glass Phys. Chem.*, 2010, vol. 36, no. 4, p. 455.

44. Kitaigorodskii, A.I., Glass structure and methods of its investigation by means of X-ray structural analysis, *UFN*, 1938, vol. 19, no. 2, p. 201.

45. http://www.netzsch-thermal-analysis.com/.

46. Sherwood, P.M.A., Briggs, D., and Seah, M.P., *Practical Surface Analysis by Auger and X-ray Photoelectron Spectroscopy,* New York: Wiley, 1983.

47. Astafiev, E.A. and Shkerin, S.H., Instruments for impedance measurement: the relationship of price-quality-functionality, *Al'tern. Energ. Ekol.*, 2008, vol. 58, p. 150.

48. Olivier, M., Tchahame, J. C., Němec, P., Chauvet, M., Besse, V., Cassagne, C., Boudebs, G., Renversez, G., Boidin, R., Baudet, E., and Nazabal, V., Structure, nonlinear properties, and photosensitivity of $(GeSe_2)_{100-x}(Sb_2Se_3)_x$ glasses, *Opt. Mater. Express*, 2014, vol. 4, p. 525.

49. Tveryanovich, Yu.S., Aleksandrov, V.V., Murin, I.V., and Nedoshovenko, E.G., Glass-forming ability and cationic transport in gallium containing chalcogenide glasses, *J. Non-Cryst. Solids*, 1999, vols. 256–257, p. 237.

50. Bychkov, E.A., Tveryanovich, Yu.S., and Vlasov, Yu.G., Ion conductivity and sensors, *Semicond. Semimetals*, 2004, vol. 80, p. 103.

Translated by T. Safonova

SPELL: 1. ok